

DEVELOPMENT OF A “NUMERICAL HAM” MODEL THAT COUPLES WATER AND SALT TRANSFERS TO PROTEOLYSIS DURING THE DRY-CURED HAM PROCESS

Harkouss R.^(a), Chevarin C.^(a), Daudin J.D.^(a), Mirade P.S.^(a)

^(a)INRA, UR370 Qualité des produits Animaux, F-63122 Saint-Genès-Champanelle, France

^(a)Pierre-Sylvain.Mirade@clermont.inra.fr

ABSTRACT

Since salting is essential during the dry-cured ham process, reducing salt content could affect the final product quality. The aim of this study was to build a 3D multi-physical numerical model which estimates the biochemical evolution (proteolysis) as well as the distribution of salt and water contents during all the stages of dry-cured ham process. The model built showed a very good prediction of the distribution of salt and water content in the ham. Its robustness was evaluated by comparing the predicted values of proteolysis index (PI) at the end of post-salting stage with the experimental PI values measured in samples extracted from industrial Bayonne hams. The 3D “numerical ham” built can be considered as an original software tool that could be helpful for professionals to reduce the final salt content in dry-cured hams.

Keywords: dry-cured ham, multi-physical numerical model, proteolysis, water and salt transfers

1. INTRODUCTION

In the dry-cured ham elaboration process which includes salting (duration of about 15 days), post-salting (8 weeks), pre-drying (1 week) and drying (5 to more than 18 months) stages, salt is a multifunctional element that influences the final product in terms of quality and safety. Salt contributes to water holding capacity, texture and flavour development and limits the growth of pathogens and spoilage microorganisms (Taormina 2010). On the other hand, the final dry-cured ham quality is also affected by the time-course of proteolysis which depends on various factors, such as temperature, pH, salt and water contents (Toldrá and Flores 2000; Arnau, Guerrero, and Gou 1997).

Although salt is essential during the dry-cured ham manufacturing, many efforts have been made to reduce the final salt content, without altering the final dry-cured ham quality. To achieve this, NaCl reduction was mainly performed through two different approaches: (a) direct reduction of NaCl content or (b) partial substitution of NaCl by other salts. Results of the first approach showed that longer post-salting time was needed for lower-sodium hams to reach the same a_w values as hams normally salted with 100% NaCl. No more than 25% salt reductions can be obtained using

this first approach. However, particular caution has to be paid when using this approach to avoid any microbiological stability problem and final defective texture as a result of abnormal proteolysis (Desmond 2006). Given these concerns, NaCl substitution by KCl, CaCl₂, MgCl₂ or K-lactate constitutes the second approach that can be used.

In food industry, salting and drying are mass transfer processes leading to time-variable water and salt content profiles. It is of high interest to assess the time-course evolution and to quantify these two parameters, e.g. to better understand their effects on the biochemical evolution and textural properties that occur during the dry-cured ham manufacture. To achieve this, numerical modelling and simulation could be a good candidate since it is non-invasive, non-destructive, less expensive, and rapid. However, very few studies aimed at modelling salt and water transfers during the different stages of dry-curing hams. On the other hand, there has not been a single study that predicted the time-course of proteolysis during the dry-cured ham production process. Very recently, Harkouss, Safa, Gatellier, Lebert, and Mirade (2014) established phenomenological models allowing proteolysis to be quantified, for five various pork muscles, as a function of temperature, water and salt content. However, quantitative modelling of salt diffusion, water migration, heat transfer and proteolysis evolution using finite element method has, to our knowledge, never been attempted in dry-cured ham. On account of this, this study aims at presenting a multi-physical 3D model developed under the Comsol® Multiphysics software that combines a determination of proteolysis through the phenomenological models developed by Harkouss et al. (2014) with salt penetration, water migration and heat transfer modelling. For practical reason, this paper is focused on the modelling of what happens in terms of water and salt transfers and proteolysis during the first stages of the dry-curing ham process, those carried out at low temperature: the salting and post-salting stages.

2. MATERIALS AND METHODS

Before integrating the proteolysis model and the heat and mass transfer models into the multi-physical model built using Comsol® multiphysics software, complete 3D ham geometry was built.

2.1. 3D Ham Geometry and Meshing

The process of constructing an accurate 3D ham representation required a series of 2D slices of a fresh ham that can be typically provided by Computed Tomography (CT), which is a rapid and non destructive X-ray imaging technique. Automated tools for noise reduction, smoothing and contrast sharpening were used as well as other data manipulation tools such as re-sampling and rescaling. The process was automated by thresholding, meaning that the different parts of the ham, i.e. rind, muscles, bone and thin film of fat between the SM and BF muscles, were identified by specifying minimum and maximum values for the signal. In total, the segmentation of 181 X-ray CT images of green ham was made using specific software called Mimics® (Materialise, Leuven, Belgium). The segmented objects were then simultaneously connected and meshed based on an orthotropic grid intersected by interfaces defining the boundaries.

The obtained 3D ham geometry was then smoothed and meshed many times in order to obtain a high quality surface mesh. After that, a volumetric tetrahedral mesh with extra smooth boundary was obtained. Finally, the 3D ham model consisting in 202,000 tetrahedral meshes and containing 5 different groups of muscle was imported into Comsol® Multiphysics software (Figure 1).

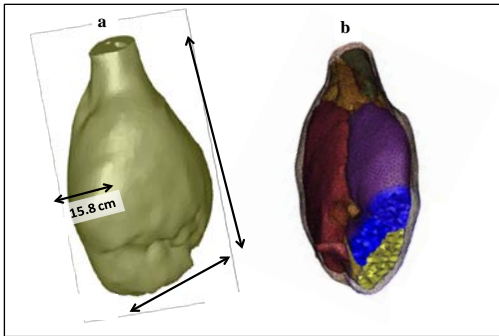


Figure 1: Views of (a) the 3D Ham Geometry Built and (b) the Volumetric Tetrahedral Mesh with the Different Groups of Muscle inside the Ham.

2.2. Model of Proteolysis

Several phenomenological models allowing proteolysis rate to be quantified as a function of several factors have been built and recently published in Harkouss et al. (2014). In the present study, modelling of proteolysis was performed from solving equation (1) and assuming that the proteolysis rate could be calculated at each time step from a global phenomenological model corresponding to Equation (2):

$$\frac{dPI}{dt} = R_i \quad (1)$$

With

$$R_i = 8.286 \cdot 10^{-4} - 1.024 \cdot 10^{-2} \cdot T + 1.147 \cdot 10^{-4} \cdot S + 1.466 \cdot 10^{-4} \cdot W - 2.62 \cdot 10^{-4} \cdot T \cdot S + 3.254 \cdot 10^{-4} \cdot T \cdot W - 1.746 \cdot 10^{-6} \cdot S \cdot W \quad (2)$$

where PI is the proteolysis index (%), T is the temperature (°C), S is the salt content (kg salt.kg dried matter⁻¹ or % DM) and W is the water content (kg water.kg total matter⁻¹ or % TM).

These two equations were solved in all domains of the numerical ham, except the bone which was logically excluded from the PI calculation. Besides, an initial condition was applied to PI. Indeed, a PI value of 2.5% was considered at time zero, which represents the mean average of a huge number of experimental PI measurements carried out on fresh small pork meat samples prepared from different ham muscles.

2.3. Heat Transfer Modelling

Fourier law was introduced to numerically simulate heat transfer inside the ham and predict how ham temperature changes in response to the modification of air temperature during the pre-drying or drying/ripening stages. The simplified equation that was solved for calculating the distribution of the ham temperature T as a function of space and time is:

$$\rho c_p \frac{\partial T}{\partial t} = \nabla \cdot (k \nabla T) \quad (3)$$

where t is the time (s), ρ is the ham density (1072 kg.m⁻³), c_p is the ham specific heat capacity (3200 J.kg⁻¹.K⁻¹) and k is the ham thermal conductivity (0.45 W.m⁻¹.K⁻¹).

This equation was applied and solved in all domains of the numerical ham, except the bone which was considered as thermally insulated. At time 0, i.e. at the beginning of the salting stage, we assumed that a green ham having an initial temperature of 3°C was placed in a cold room with air at 4°C.

At the air-ham interface, the following thermal boundary condition was imposed in the model, thus allowing the heat flow rate q to be calculated taking into account the thermal convection and the energy exchanged during water evaporation:

$$q = h (T_{air} - T_{surface}) + \varphi_{water} \cdot L_v \quad (4)$$

In equation (4), h represents the convective heat transfer coefficient. A value of h equal to 7 W.m⁻².K⁻¹ was considered in the present model as a result of low air velocity (Kondjoyan and Daudin 1997). $T_{surface}$ represents either the temperature of the muscle surface where salt is added or the temperature of the ham rind surface where no salt is added since we modelled here a “limited salt input” salting procedure consisting in salting only the muscle part of the ham without salting the rind. At last, in equation (4), L_v represents the latent heat due to the water evaporation (equal to 2450 kJ.kg⁻¹) and φ_{water} is the water flow rate that evaporates from the muscle or the rind surface (please see Equation (5)).

2.4. Mass Transfer Modelling

We assumed that the mass transfer phenomena that occur during the dry-cured ham elaboration process, i.e.

salt diffusion and water migration, can be modelled by the following Fick equation:

$$\frac{\partial c_i}{\partial t} + \nabla \cdot (-D_i \nabla c_i) = 0 \quad (5)$$

where c_i is the salt or water concentration. In equation (5), D_i represents the diffusion coefficient of salt or water inside the ham. For these coefficients, in the lean meat of ham, we assumed a constant D_{salt} equal to $5 \cdot 10^{-10} \text{ m}^2 \cdot \text{s}^{-1}$, but a D_{water} varying as a function of the water content expressed on dry basis (X_{water}) according to the following relation (Ruiz-Cabrera et al. 2004):

$$D_{\text{water}} = 4 \cdot 10^{(0.625 \cdot X_{\text{water}} - 12)} \quad (6)$$

The Fick equation was solved in all domains, except in the bone which was logically excluded from the calculation. An initial salt content of 0% TM and an initial water content of 75% TM, i.e. values corresponding to fresh meat, were imposed in the model.

As previously indicated, the “numerical ham” model was used first to assess what happens in terms of water and salt transfers and proteolysis during the first 11 weeks of process performed at low air temperature. This period of time included a first stage of salting corresponding to a “limited salt input” salting procedure applied for 15 days. From a numerical point of view, salting on the muscle side was modelled through the application of a brine solution composed of a variable mass of salt added to a constant volume of water. Indeed, at each time step of the salting stage, the mass of salt that penetrated inside the ham was calculated as well as the mass of salt that stayed at the ham surface and thus the new salt concentration of the brine solution in contact with the muscle side of the ham. The salting stage was then followed by 62 days of post-salting during which salt diffused inside the ham. Simultaneously to salt diffusion, water migration occurred from inside the ham to the outer zones where evaporation took place. For that purpose, specific boundary conditions had to be imposed at the ham-air interface in terms of mass flow rates. The water flow rate can be calculated from the following equation:

$$\varphi_{\text{water}} = k \cdot \left(a_{w,\text{surface}} \cdot P_{\text{sat},T_{\text{surface}}} - \frac{RH_{\text{air}}}{100} \cdot P_{\text{sat},T_{\text{air}}} \right) \quad (7)$$

with an air relative humidity value RH_{air} of 70% and in the range of temperature 0-40°C:

$$P_{\text{sat},T} = \exp \left(-\frac{6764}{T} - 4.915 \cdot \log T + 58.75 \right) \quad (8)$$

In equation (7), k , which is the water transfer coefficient ($\text{kg} \cdot \text{m}^{-2} \cdot \text{Pa}^{-1} \cdot \text{s}^{-1}$), can be calculated from the convective heat transfer coefficient h using the relation:

$$k = \frac{h \cdot M_{\text{water}}}{Cp_{\text{air}} \cdot M_{\text{air}} \cdot P_{\text{atm}} \cdot Le^{2/3}} \quad (9)$$

with $M_{\text{water}} = 18 \text{ g} \cdot \text{mol}^{-1}$; $Cp_{\text{air}} = 1004 \text{ J} \cdot \text{kg}^{-1} \cdot \text{K}^{-1}$; $M_{\text{air}} = 29 \text{ g} \cdot \text{mol}^{-1}$; $P_{\text{atm}} = 1 \text{ atm}$; and Le is the Lewis number which is equal to 0.777, for air. On the rind side of the ham, we arbitrary assumed that the water transfer coefficient k was divided by a factor 20 to indirectly account for the barrier effect against water transfer played by the fat layer located just under the rind.

In equation (7), the term ‘surface’ is associated either to the muscle side or to the rind side, depending on the boundary condition considered. On the rind side of the ham, we arbitrary considered that a_w was equal to 1 due to the presence of a few mm-thick fat layer. On the other hand, on the muscle side of the ham, owing to the presence of salt, a_w at the muscle surface obeyed to the following relations (Rougier et al. 2007):

$$a_{w,\text{salted meat}} = a_{w,\text{meat with no salt}} \cdot a_{w,\text{salted water in meat}} \quad (10)$$

with

$$a_{w,\text{meat with no salt}} = 0.993 \cdot \exp(-0.0204 \cdot X_{\text{water}}^{-1.96}) \quad (11)$$

$$a_{w,\text{salted water}} = -0.4553 \cdot X_{\text{salt}}^{\text{water}^2} - 0.5242 \cdot X_{\text{salt}}^{\text{water}} + 0.999 \quad (12)$$

where $X_{\text{salt}}^{\text{water}}$ represents the salt content expressed on water basis ($\text{kg salt} \cdot \text{kg water}^{-1}$).

In terms of salting, the boundary condition applied to the muscle side of the ham consists in writing the equality of water activities between the brine solution and the first layer of meat in contact with this brine solution. This assumption leads to:

$$a_{w,\text{brine solution}} = a_{w,\text{salted meat}} \quad (13)$$

The first term of this equation was calculated using equation (12) and from the salt balance performed at each time step of the salting stage on the salting surface allowing the mass of salt to be calculated and thus, for the brine solution, the term $X_{\text{salt}}^{\text{water}}$. The right-hand-side term of equation (13) corresponds to equation (10). Solving equation (13) allows, for the salted meat, the term $X_{\text{salt}}^{\text{water}}$ to be assessed, and then the salt concentration in the first layer of meat in equilibrium with the brine solution.

2.5. Solving of Equations

Once implemented in the “numerical ham” model, solving all these equations lasted about 3.5 h on a 3 GHz Xeon 8-processors PC with 48 Go of RAM to model what happened during the salting and post-salting stages in terms of time course of proteolysis and water and salt transfers, with a time step of 0.1 day.

3. RESULTS AND DISCUSSION

Here only the results corresponding to the first two stages performed at low temperature, i.e. salting and post-salting, will be shown.

3.1. Distribution of Spatial and Time Values of Salt Content, Water Content and PI

Figure 2 shows the distribution of PI, water and salt contents predicted by the numerical model during the salting stage, after one week or two weeks of process.

In this figure, each view presents the distribution of water content, in the range 50%-75% TM, on the section located in the lower part of the ham geometry, the distribution of salt content, in the range 0%-10% TM, on the section located in the middle part of the ham geometry, and that of PI, in the range 2.5%-12.5%, on the section located in the upper part of the ham geometry. After one week of process, the salt penetration is only visible in the few first centimetres from the salting surface, leading to a salt concentration reaching 10% TM in this region, whereas it is lower in the middle part of the ham (2%-3% TM) and negligible near to the rind side of the ham opposite the salting surface. Concerning the water migration and distribution, Figure 2 shows that just the superficial area of the “muscle side” of the ham has lost water during the first week of process.

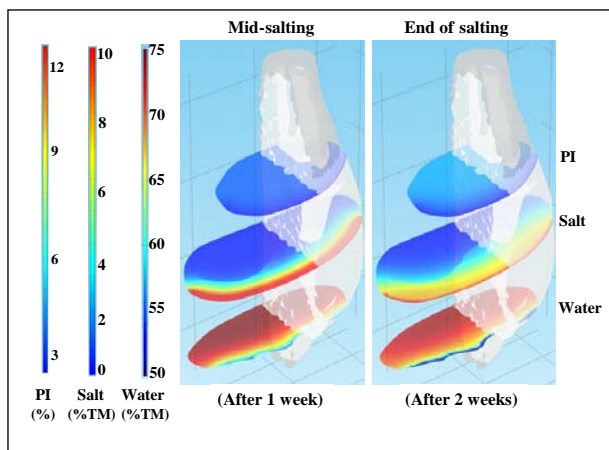


Figure 2: Distribution of PI, Salt and Water Contents Predicted during the Salting Stage, at Mid-Salting and at the End of Salting

After two weeks of process, i.e. at the end of salting, Figure 2 shows that salt has diffused more inside in the ham, increasing obviously the salt concentration, in particular in the middle part of the ham where concentration values reach 5% TM; however, the salt concentration is still relatively low in the deeper zones of the ham. Due to water evaporation, the water content of the ham continued to decrease until the end of salting, but this is still visible close to the salting surface, in particular in the few first millimetres of this surface where the water content decreased to 55% TM. As a result of the short duration of process, PI values did not increase clearly during these two weeks, even if, in the deeper zones of the ham, predicted PI was equal to approximately 4-5% compared to 2.5%-3% close to the salting surface. Actually, owing to the behaviour highlighted by the phenomenological models of proteolysis built, the predicted PI values were

logically lower in areas highly dried and highly salted, as close to the salting surface. Inside the ham, the proteolysis logically increased due to high water content values combined to low salt content values, thus leading to a 2-3% increase in PI values during the two first weeks of process (Figure 2).

During the post-salting stage, numerical simulation showed that, some weeks after the end of salting, homogeneity started to take place in the different domains of the ham (Figure 3). This homogeneity is more and more visible, especially when visualizing the distribution of salt content at the end of the post-salting stage. During this stage, salt showed a great ability to penetrate deeply towards the inner zones of the ham. After six weeks, the salt content gently increased in the middle of the ham (4%-5% TM) and slightly in the deepest zones of the ham where values of 2%-3% TM were predicted. Meanwhile, the water content of the ham gradually decreased in the inner zones (68%-70% TM) and the very dried zone still exists close to the salting surface. Due to the evolution of the salt and water content, PI values logically increased inside the ham where indices ranging from 7% to 9% were predicted, leading to the apparition of a gradient of PI between the inner zone of the ham and the zone located in close proximity to the salting surface where salting and drying highly inhibited the proteolysis evolution.

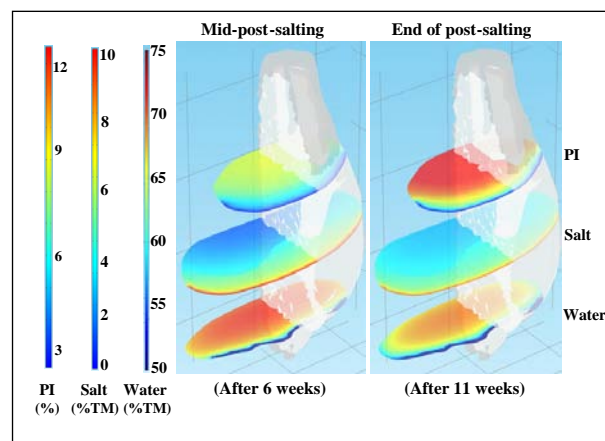


Figure 3: Distribution of PI, Salt and Water Contents Predicted during the Post-Salting Stage, at Mid-Period and at the End of Post-Salting

At the end of the post-salting stage, i.e. after 11 weeks of process, due to diffusion, the distribution of salt appeared as more and more homogeneous inside almost all the ham volume with values of salt content of about 4-5% TM. The salt content even decreased in the zone close to the salting surface where high salt content values were now predicted only on the few first millimetres (Figure 3). During this period, the water content obviously decreased inside the ham (65%-67% TM) and the thickness of the very dried zone close to the salting surface slightly increased (Figure 3). Eleven weeks were finally necessary to raise the predicted PI values in a noticeable manner, especially in the inner domains of the ham where PI exceeded 10%. Figure 3

also shows that a gradient of PI is created between the surface where salt was deposited and the inner zones of the ham.

3.2. Predicted Mean Values of Salt Content, Water Content, PI, and a_w

The “numerical ham” model also allows calculating mean values of the predicted parameters, such as salt content, water content, PI and a_w in the different groups of muscles identified in the ham geometry during its construction using Mimics® software.

Figure 4 shows the time course of mean values of salt content predicted by the “numerical ham” model during the salting and post-salting stages in three different groups of muscles: (1) in the SM muscle, called “grosse noix” in a “French butcher” language, (2) in the ‘BF + ST’ muscles, called “sous-noix” in a “French butcher” language, and (3) in all the ham volume. Due to salting, the salt content in these three different groups of muscles increased rapidly, especially since the group of muscles is located close to the salting surface. That is why the salt content in the SM muscle increased more rapidly and exceeded 6% TM, in average, at the end of salting compared to the one of the “sous-noix” whose mean value reached about 1% TM over the same period. During the post-salting stage, the salt content of the group of muscles close to the salting surface decreased in favour of the one located inside the ham, due to diffusion (Figure 4).

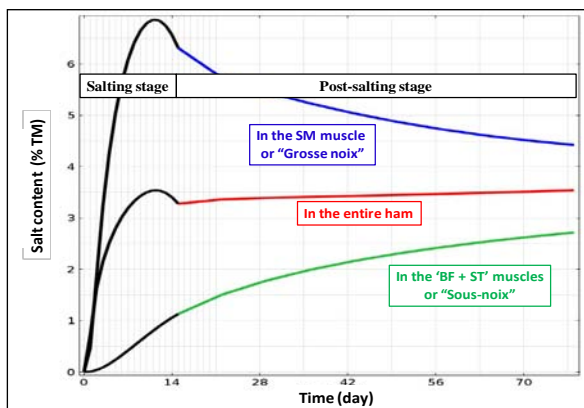


Figure 4: Time Course of Mean Values of Salt Content Predicted during the Salting and Post-Salting Stages and Calculated in the SM Muscle, in the ‘BF + ST’ Muscle and in the Entire Ham

Regarding the entire ham, the behaviour in terms of time course of salt content was logically intermediate compared to the two other groups of muscles, with a mean value equal to 3.3% TM at the end of the salting stage. This value of salt content then increased slightly during the post-salting stage due to the water evaporation which led to a concentration of salt. Salt content in the entire ham thus reached 3.5% TM, after 77 days of process (Figure 4).

Figure 5 shows the time course of mean values of water content predicted by the model during the salting and post-salting stages in the three same groups of

muscles than for salt diffusion. Due to water evaporation, the predicted water content in these three groups of muscles logically decreased, but more or less rapidly according to their distance from the ham surface. Since the “muscle side” surface dried more rapidly than the “rind side” surface of the ham, the water content in the “grosse noix” decreased more rapidly than in the “sous-noix”. The difference in water content between these two groups of muscles reached 6% TM, in average, at the end of the post-salting stage. As previously, the behaviour of the entire ham in terms of decrease in water content was intermediate when comparing to the two other groups of muscles, thus leading to a final mean value of water content in the entire ham equal to 66% TM, after 77 days of process.

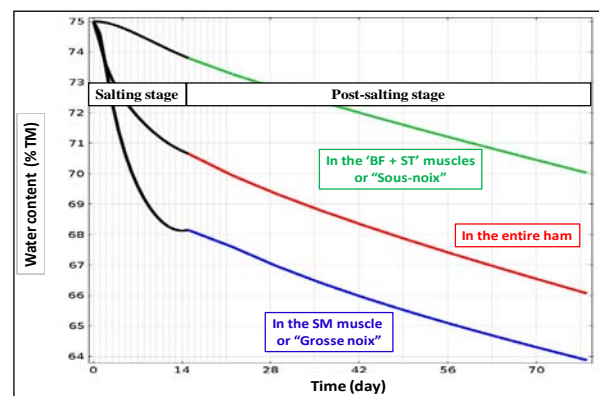


Figure 5: Time Course of Mean Values of Water Content Predicted during the Salting and Post-Salting Stages and Calculated in the SM Muscle, in the ‘BF + ST’ Muscle and in the Entire Ham

Figure 6 shows the evolution of mean values of PI predicted over the 77 days period in the “grosse noix”, the “sous-noix” and in the entire ham, from the phenomenological models implemented in the model. Since the temperature has not changed during the two stages modelled here, the predicted mean values of PI were directly linked to the time course of salt content and water content previously described. So the lower mean values of PI were predicted in the most dried and salted group of muscles, i.e. the “grosse noix”. The difference in PI values exceeded 3% between the “sous-noix” (12.5%) and the “grosse noix” (9%); the mean PI value of the entire ham was intermediate (10.7%). In fact, these calculated PI values globally were in agreement with those measured on samples extracted from two types of muscle (BF and SM) of industrial Bayonne dry-cured hams, at the end of the post-salting stage. The experimental PI values were equal to $12\% \pm 1\%$ and $9\% \pm 1\%$ for BF and SM, respectively, i.e. values which are relatively close to the calculated PI, thus demonstrating the accuracy of prediction of the 3D “numerical ham” model built. Accurate analysis of results reveals that the difference in terms of time course of mean values of PI between the 3 groups of muscles appeared early in the second or third day of salting.

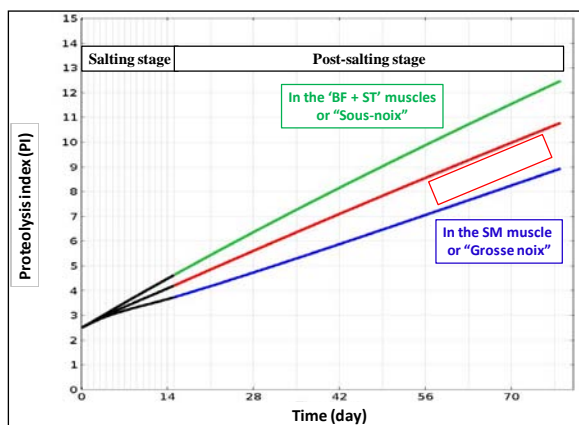


Figure 6: Time Course of Mean Values of PI Predicted during the Salting and Post-Salting Stages and Calculated in the SM Muscle, in the 'BF + ST' Muscle and in the Entire Ham

Figure 7 shows the time course of mean values of a_w predicted during the salting and the post-salting stages in the "grosse noix", in the "sous-noix" and also in the entire ham. The increase of salt content in the muscles combined to the decrease in the water content due to drying globally led to a decrease in mean a_w values in all the groups of muscles with the objective of reaching the microbial stability, which is the aim of the salting and drying operations performed during the dry-cured ham process. It can be noted, in Figure 7, the mean a_w value of the "grosse noix" increased during the post-salting stage as a result of an increase in a_w due to the salt diffusion from the "grosse noix" to the "sous-noix" as shown in Figure 4 not counterbalanced by the decrease in a_w due to the drying that occurred at the same period. However, the mean value of a_w in the entire ham decreased progressively during the post-salting stage, from 0.96, after 15 days, to 0.955, at the end (Figure 7).

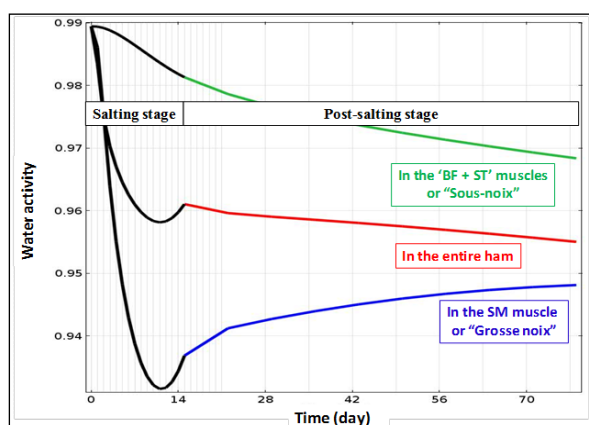


Figure 7: Time Course of Mean Values of a_w Predicted during the Salting and Post-Salting Stages and Calculated in the SM Muscle, in the 'BF + ST' Muscle and in the Entire Ham

4. CONCLUSION

This study presented the development of a numerical model that simulates water and salt transfers in a real ham, and couples the time course prediction of the salt and water content to PI evolution through the implementation of a specific phenomenological model established in a previous study. The present "numerical ham" model is able to predict the time course of salt and water content, PI, and a_w , and profiles can be extracted anywhere in the ham to make the interpretation of the phenomena easier to understand. However, this model needs to be more validated by performing an accurate comparison of the predicted values of salt and water content, and of a_w with experimental values.

To the authors' knowledge, a complete 3D multiphysical numerical model of dry-cured ham was built for the first time. This "3D numerical ham" model constitutes a new numerical tool that would be greatly useful for helping industrials to investigate various process scenarios in order to reduce the final salt content of dry-cured hams, without modifying their final quality in terms of proteolysis, texture and flavour.

ACKNOWLEDGMENTS

This work was funded by the Na- integrated programme (ANR-09-ALIA-013-01) financed by the French National Research Agency. We thank IFIP for providing CT images.

REFERENCES

- Arnau, J., Guerrero, L., Gou, P., 1997. Effects of temperature during the last month of ageing and of salting time on dry-cured ham aged for six months. *Journal of the Science of Food and Agriculture*, 74, 193-198.
- Harkouss, R., Safa, H., Gatellier, P., Lebert, A., Mirade, P.S., 2014. Building phenomenological models that relate proteolysis in pork muscles to temperature, water and salt content. *Food Chemistry*, 151, 7-14.
- Kondjayan, A., Daudin, J.D., 1997. Heat and mass transfer coefficients at the surface of a pork hindquarter. *Journal of Food Engineering*, 32, 225-240.
- Rougier, T., Bonazzi, C., Daudin, J.D., 2007. Modelling incidence of lipid and sodium chloride contents on sorption curves of gelatine in the high humidity range. *LWT- Food Science and Technology*, 40, 1798-1807.
- Ruiz-Cabrera, M., Gou, P., Foucat, L., Renou, J.P., Daudin, J.D., 2004. Water transfer analysis in pork meat supported by NMR imaging. *Meat Science*, 67, 169-178.
- Taormina, P.J., 2010. Implications of salt and sodium reduction on microbial food safety. *Critical Reviews in Food Science and Nutrition*, 50, 209-227.
- Toldrá, F., Flores, M., 2000. The use of muscle enzymes as predictor of pork meat quality. *Food Chemistry*, 69, 387-395.